PFC/RR-86-12 DOE/ET-51013-182

STRUCTURAL PROPERTIES OF REINFORCED COPPER

H. Becker, M. Besen, E. Bobrov, J. Chen,
and D.B. Montgomery, Massachusetts Institute
of Technology/Plasma Fusion Center
D. Tognarelli and R. Walty, Manlabs

SUMMARY

Exploratory experimental studies were performed, and simple prediction procedures were developed, to determine Young's moduli and yield strengths of reinforced copper under inplane tension and under face compression. The predictions are compared with the test data. Agreement appears to be good enough to support the hypothesis that those properties can be predicted by mixture rules. For the near-term, it appears reasonable to employ the prediction procedures in Compact Ignition Magnet design. However, more testing is required to increase confidence in use of the procedures. An example illustrates application of the method to CIT magnet coil design.

The primary purpose of the study has been to explore the structural response of reinforced-copper laminated composites when subjected to face compression. Perhaps the most important results obtained so far are the observations that the reinforced copper withstood face pressures much greater than the copper yield strength, and that the copper did not extrude laterally.

TABLE OF CONTENTS

FIGURES

TABLES

SYMBOLS

b = arbitrary length

E = Young's modulus:

- E_c - copper
- E_i - composite under inplane tension
- E_f - composite under face compression
- E_r - reinforcement

E_t = Tangent modulus

- $E_{t,c}$ - copper
- $E_{t,i}$ - composite under inplane tension
- $E_{t,f}$ - composite under face compression
- $E_{t,r}$ - reinforcement

E-B = Explosion-bonded (Composite)

L = Length of edge shear zone on finite width plate

R = Aspect ratio of copper in stack, w/t_c

R-B = Roll-bonded (composite)

t_c = Total Thickness of copper component in composite

t_r = Total Thickness of reinforcement component in composite

w = Width of square plate in stack

X_i = Numerical value of i-th quantity in statistical analysis

α = $t_c/(t_c + t_r)$

ε = Strain

- ε_c - in copper, through thickness
- ε_r - in reinforcement, through thickness
- ε_i - general inplane
- $\varepsilon_{c,i}$ - inplane in copper
- $\varepsilon_{r,i}$ - inplane in reinforcement

ϕ = $\sigma'_{f,y}/\sigma_{f,y}$

μ = Average of several numerical quantities

σ = Stress

σ_f - face compression

σ_i - inplane tension

$\sigma_{c,i}$ - inplane in copper

$\sigma_{r,y}$ - inplane in reinforcement

$\sigma_{c,y}$ - copper yield

$\sigma_{f,y}$ - face compression yield for infinite plate (mixture rule value)

$\sigma_{i,y}$ - inplane tension yield

$\sigma_{r,y}$ - reinforcement yield

$\sigma'_{f,y}$ - face compression yield for finite width plate

σ_t - tresca, $\sigma_f - \sigma_c$ in copper, $\sigma_f - \sigma_r$ in reinforcement (algebraic signs: + = tension in component, - = compression)

$\parallel$ = Parallel to interface wave ridges

$\perp$ = Perpendicular to interface wave ridges

INTRODUCTION

Background

Compact Ignition Magnets are being designed with copper conductors. The high central toroidal fields (9 to 10 tesla) induce fields of the order of 20 tesla at the outer radii of the inner legs on the TF coil. The average toroidal compression stresses are in the 450 MPa range. The free-standing OH coil has a 24 tesla field inside the winding, which induces average toroidal tension stresses of 440 MPa. The fields from the PF coil system induce vertical compression equal to 80 MPa.

This situation requires a conductor with high strength. It also requires good electrical conductivity to minimize temperature rise during a pulse. One method of producing plates with that combination is to generate a composite structure by bonding high conductivity copper to a high strength metal such as Inconel (or perhaps stainless steel). The structural properties of such a combination have been explored in both inplane tension[1,2], and in face compression[3], in connection with magnet design. The tests of Reference 3 were performed on unbonded copper/steel stacks in which the components were a few mils thick and about 2 inches in diameter. Observed yield strengths were of the order of twice that of cold worked unbonded copper. That situation may exist in Alcator C, although the plate thicknesses are much greater.

Prediction of inplane behavior appears to be reasonably straightforward. However, response to face compression had not been explored enough to permit defining a design procedure. Furthermore, many magnet engineers have assumed that face compression behavior is limited by the

properties of the unreinforced copper, although evidence exists[4] to indicate that such an assumption may be overly conservative.

It is the purpose of this study to explore those types of structural behavior and to reveal the gain in face compression yield strength when copper is reinforced by a high strength metal.

Program Goals

The primary goal of the Composite Test Program is to provide structural property data for magnet coil design. In the CIT Program the TF coil will be loaded only in toroidal compression, radial compression, and vertical bending. The PF coils will be loaded in toroidal tension, vertical compression, radial compression, and possibly in vertical and radial bending. Consequently, both inplane tension and face compression data are required.

It is desirable to develop a procedure for predicting the structural behavior of the reinforced copper composite, not only as a fundamental scientific activity, but also to calculate the impact of likely design changes as the program proceeds.

Another program goal is to determine whether a predictable relation exists between the yield strengths for inplane tension and for face compression. Inplane tension tests require relatively small amounts of material. Furthermore, they can be performed quickly using more-or-less standard specimens and measurement techniques in conjunction with testing machines that produce loads in the 10,000 lb (70 KN) range. Face compression tests require large amounts of material arrayed in stacks, and loads in the Multi-Mlb (tens of MN's) range. Use of large machines for compression tests often require long lead times. Furthermore, no standards

exist for performing that type of test. As a result, there would be value in being able to perform only tension tests to obtain both tension and compression yield strength data.

Procedures

This program involves developmemt of methods for predicting composite response to inplane tension and to face compression, conduct of tests to reveal the general nature of the response, and comparison of prediction with test data. Experiments were performed on roll-bonded, explosion-bonded and unbonded composites. They included strip stress-strain tests on the composite components and on the composites, as well as face compression stress-strain tests on stacks of both bonded and loose plate segments.

A simple procedure was developed for converting component tension stress-strain curves into inplane tension stress-strain curves for a reinforced copper composite. An hypothesis was employed that led to a calculation method for face compression yield strength of an infinite plane plate. A method also was developed for estimating the strength of a finite width plate. Those procedures were combined into a method for predicting the yield strengths of the test stacks. Measured yield strengths were compared with the predictions for eight stacks with widely varying properties. The measured compression yields also were compared with the measured tension yields of four bonded composites.

The results of the comparisons led to the conclusions at the end of the report. Planned continuation activities also are presented.

ANALYSES OF STRUCTURAL BEHAVIORS

Introduction

The following strength-of-materials analyses have been developed to identify the structural interaction of the copper and reinforcement in a composite, and to offer a relatively simple method of estimating the structural behavior under inplane tension and under face compression. Finite element calculations have been attempted to identify face compression behavior. However, to date they do not correlate with the test data. No comparison is presented in this report. That analysis activity is expected to continue and will be reported when good correlation is achieved with test results.

Elastic Moduli

The copper and reinforcement of the composite are considered to be united so that the inplane strains in the copper match the inplane strains in the reinforcement throughout the composite (Fig. 1a). Furthermore, the inplane forces in the copper and reinforcement are balanced in the direction perpendicular to an inplane tension load (Fig. 1b), or in both inplane directions perpendicular to a face compression load (Fig. 1c).

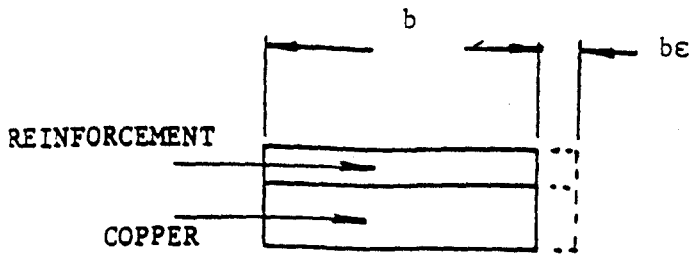

a. INPLANE STRAIN MATCH

b. INPLANE FORCE BALANCE DUE TO INPLANE LOAD

c. INPLANE FORCE BALANCE DUE TO FACE LOAD

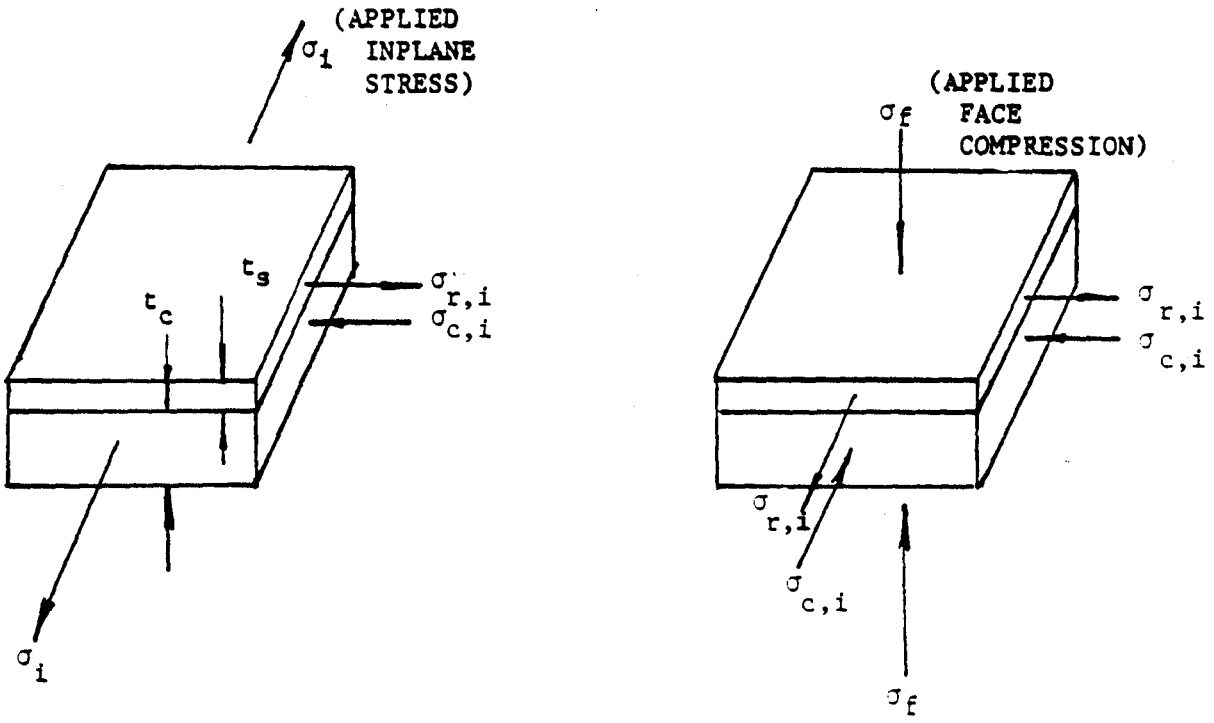

Figure 1. Stresses and Strains in Composite Components.

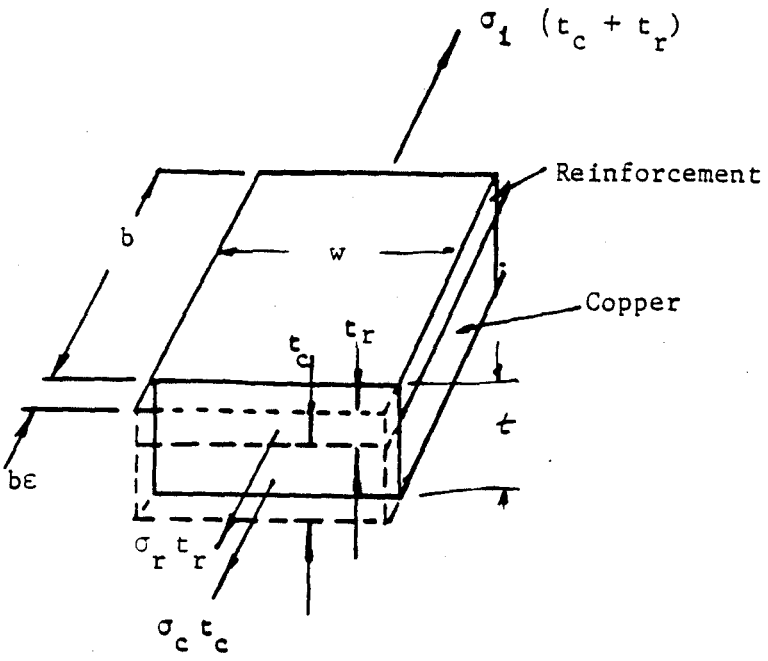

$$\sigma_i(t_c + t_r) = \sigma_{c,i}\ t_c + \sigma_{r,i}\ t_r \qquad \text{(a)}$$

$$\text{or with } \alpha = t_c/(t_c + t_r) \qquad \text{(b)}$$

$$\sigma_i = \alpha\sigma_{c,i} + (1 - \alpha)\sigma_{r,i}$$

$$\varepsilon_i = \sigma_{c,i}/E_c = \sigma_{r,i}/E_r \qquad \text{(c)}$$

$$E_i = \sigma_i/\varepsilon_i = \alpha E_c + (1 - \alpha)E_r \qquad \text{(d)}$$

Figure 2. Derivation of Parallel Mixture Rule for Elastic Narrow Composite Under Inplane Tension

For determination of the inplane Young's modulus, it is assumed that Poisson's ratio is the same for the composite components. As a result, the lateral strains would be the same in each component from the portion of applied load that it carries. In that case, no transverse forces would exist and the inplane elastic modulus could be determined by a simple parallel mixture rule (Fig. 2),

$$E_i = \alpha E_c + (1 - \alpha)\, E_r \tag{1}$$

If the interfaces were not united, and were frictionless in addition, the simple series mixture rule

$$1/E_f = \alpha/E_c + (1 - \alpha)/E_r \tag{2}$$

would apply to face compression as shown in Fig. 3a. However, the behavior of a united composite under elastic face compression would be more complex (Fig. 3b). The face compression, σ, would be the same on both components. Consequently, the copper inplane Poisson expansion, $\nu\sigma_f/E_c$, would exceed that of the steel, $\nu\sigma_f/E_s$. This would induce equi-biaxial inplane tension in the steel and compression in the copper such that the inplane forces would balance in both inplane directions. As can be seen in Fig. 3b, the effective Young's modulus for face compression would be found from

$$1/E_f = \alpha/E_c + (1 - \alpha)/E_s - \frac{2\nu^2\alpha(1 - \alpha)(1 - E_c/E_s)^2}{(1 - \nu)E_c\,(1 - \alpha + \alpha E_c/E_s)} \tag{3}$$

The first two terms are the same as the RHS of Eq. (2). The third term will vanish when $\alpha = 1$ or 0. It would be small in any case. For example, if $\nu = 0.3$, $\alpha = 0.5$, and $E_c/E_s = 1/2$, then the term would be equal, approximately, to $0.02/E_c$, which would have little effect on E_f.

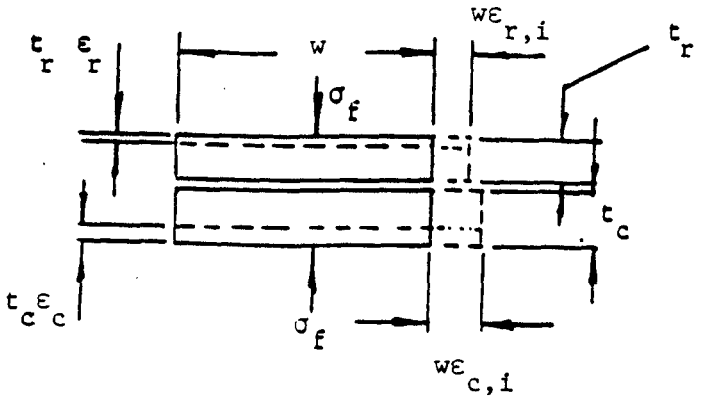

At $\nu = \nu_s = \nu_c$,

$\varepsilon_r = \sigma_f/E_r$

$\varepsilon_c = \sigma_f/E_c$

$\bar{\varepsilon}_r = \nu\sigma_f/E_r$

$\bar{\varepsilon}_c = \nu\sigma_f/E_c$

$$(t_s + t_c)\varepsilon_f = t_c\varepsilon_c + t_r\varepsilon_r \tag{e}$$

$$1/E_f = \varepsilon_f/\sigma_f = \alpha/E_c + (1 - \alpha)/E_r \tag{f}$$

a. Behavior of Frictionless Interface, Non-united Components

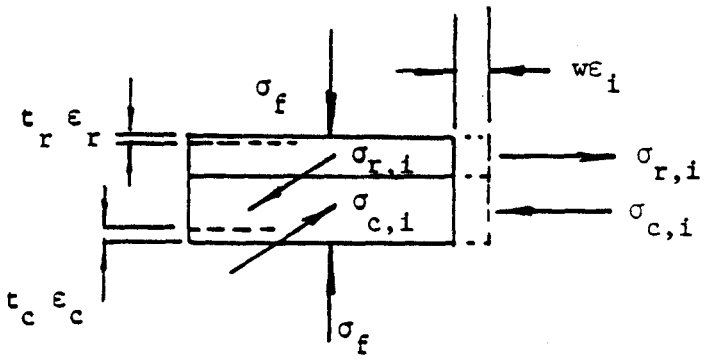

For an infinite plane plate,

$$\varepsilon_c = \sigma_f/E_c - 2\nu\sigma_{c,i}/E_c, \quad \varepsilon_r = \sigma_f/E_r + 2\nu\sigma_r/E_r \tag{g}$$

$$\varepsilon_{c,i} = \nu\sigma_f/E_c - (1 - \nu)\ \sigma_{c,i}/E_c = \nu\sigma_f/E_r + (1 - \nu)\ \sigma_r/E_r = \varepsilon_{r,i} \tag{h}$$

$$(t_c + t_s)\ \varepsilon_f = t_c\varepsilon_c + t_r\varepsilon_r \tag{i}$$

$$1/E_f = \alpha/E_c + (1 - \alpha)/E_r - \frac{2\nu^2\alpha(1- \alpha)(1 - E_c/E_r)^2}{(1 - \nu)E_c(1 - \alpha + \alpha\ E_c/E_r)} \tag{j}$$

b. Behavior of Composite

Figure 3. Derivations of Series Mixture Rules for Elastic Composites Under Face Compression.

Inelastic Moduli

The local slope of the composite stress-strain curve can be found from $E_t = d\sigma/d\varepsilon$. For inplane loads on a narrow strip (small w/t),

$$E_{t,i} = \alpha E_{t,c} + (1 - \alpha) E_{t,r} \qquad (4)$$

$E_{t,i}$ will be zero for an elastic-plastic copper in the yield range. In that case

$$E_{t,r} = E_t/(1 - \alpha) \qquad (5)$$

In any case, the parallel mixture rule would apply at all strain levels.

A wide plate (w/t >> 1) will have inplane stresses perpendicular to the load direction due to the different Poisson's ratios of the inelastic copper and the still-elastic reinforcement. The theoretical prediction of that behavior is being investigated. Intuitively, however, the tresca stress in the reinforcement could be increased because of that condition. As a result, the composite strain at any stress would be expected to increase.

Face compression tangent moduli also could be computed from $E_t = d\sigma/d\varepsilon$. In that case

$$1/E_{t,f} = \alpha/E_{t,c} + (1 - \alpha)/E_{t,r} \qquad (6)$$

However, the problem is identifying $E_{t,c}$ and $E_{t,r}$ at any stress level using the stress-strain curves of the composites. That problem also is being investigated.

It it possible to determine $\sigma_{i,y}$ from the parallel mixture rule if $E_{t,c}$ is small. Another theroretical method is to construct the stress-strain curve from the curves of the components, using the procedure described above, and then finding the 0.002 strain offset stress level.

Yield Strengths

There can be little doubt that the joining process and subsequent treatment will alter the yield strengths of the composite components. Consequently, from a practical standpoint, the best way to determine the composite inplane tensile yield (and ultimate, also) may be to measure that property on samples of the composite with component proportions in the range of anticipated design values.

Determination of the face compression yield may present a problem, as discussed below. If a relation can be established between inplane tension yield and face compression yield, the difficulty might be circumvented. There may be a basis for believing that both those yield values would be the same.

It is hypothesized that tresca yielding would occur in an infinite composite plane plate under face compression when both components yield simultaneously. That is, the tresca stress[1] in the copper would reach the uniaxial copper yield strength at the same time that the tresca stress in the reinforcement reaches the uniaxial reinforcement yield strength

---

[1] It should be noted that the equi-biaxial inplane stress field in each component, under face compression, leads to the same effective stress whether the tresca or the von Mises criterion is used.

(Fig. 4). When the inplane force balance is included, it is found that the face compression yield strength is

$$\sigma_{f,y} = \alpha\sigma_{c,y} + (1 - \alpha)\sigma_{r,y} \tag{7}$$

It is like the mixture rule for a parallel system, which could pertain to the inplane tension yield strength of the composite. That implies, that the face compression yield strength for an infinite plane plate would be the same as the inplane tension yield strength of a narrow strip.

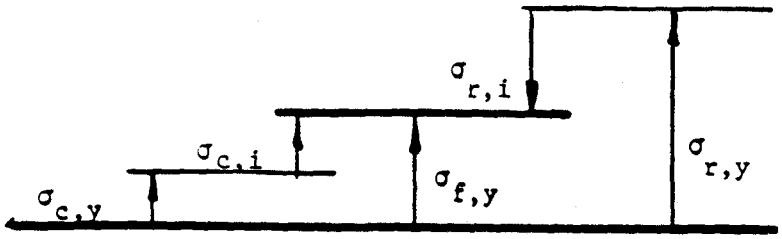

$$\sigma_{tresca}^{*} = \sigma_{f,y} \text{ (Basic Assumption)} \quad (k)$$

$$\sigma_{f,y} - \sigma_{c,i} = \sigma_{c,y} \quad (l)$$

$$\sigma_{f,y} + \sigma_{r,i} = \sigma_{r,y} \quad (m)$$

$$\sigma_c t_c = \sigma_r t_r, \text{ or } \alpha\sigma_c = (1 - \alpha)\sigma_r \quad (n)$$

$$\text{Then } \sigma_{f,c} = \alpha\,\sigma_{c,y} + (1 - \alpha)\sigma_{r,y} \quad (o)$$

* NOTE: The tresca and von Mises stresses are equal, since the inplane stresses are the same in all directions.

Figure 4. Derivation of Yield Strength Relation for an Infinite Composite Plane Plate Under Face Compression.

Effect of Finite Width on Face Compression Yield Strength

The aspect ratio, $R = w/t_c$, of the copper component will determine how closely the composite face-compression yield strength can approach the mixture rule value in Eq. (7). An estimate of the effect is developed in this section. Use is made of that procedure subsequently in comparing predictions with test data.

An important factor is the ratio of reinforcement yield strength to copper yield strength, as can be seen from the equations in Figs. 5 and 6. If $\sigma_{r,y} >> \sigma_{c,y}$, that could offset the advantage of larger R.

Figure 7 illustrates how the various parameters affect the finite width connection factor. The relations are

$$\phi = 1 - \frac{L}{w} \frac{(1 + \alpha) + (1 - \alpha)(\sigma_{r,y}/\sigma_{c,y})}{\alpha + (1 - \alpha)(\sigma_{r,y}/\sigma_{c,y})} \tag{8}$$

where

$$L/w = (L/t_c)/(w/t_c)$$

and

$$L/t_c = (0.866)(1 - \alpha)(\sigma_{r,y}/\sigma_{c,y} - 1) \tag{9}$$

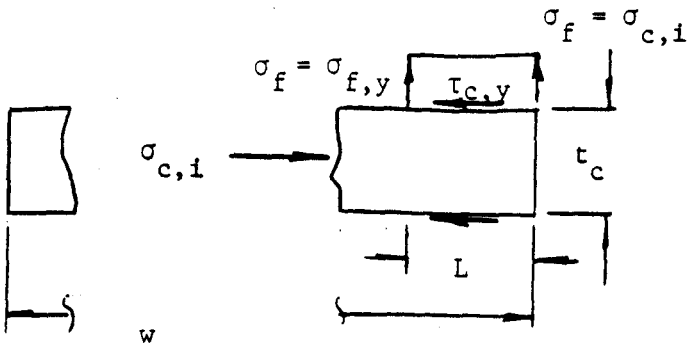

From inplane force balance,

$$2\,\tau_{c,y}L = \sigma_{c,i}t_c \qquad (w)$$

or

$$L/t_c = \sigma_{c,i}/2\tau_{c,y} \qquad (x)$$

Assume von Mises shear yield in copper,

$$\tau_{c,y} = \sigma_{c,y}/(3)^{1/2} = 0.577\,\sigma_{c,y} \qquad (y)$$

Then

$$L/t_c = 0.866\,\sigma_{c,i}/\sigma_{c,y} \qquad (z)$$

From the mixture rule,

$$\sigma_{f,y} = \alpha\sigma_{c,y} + (1 - \alpha)\sigma_{r,y} \qquad (aa)$$

The tresca criterion requires that $\sigma_{f,y} - \sigma_{c,i} = \sigma_{c,y}$ (bb)

Combine (b), (d), (e) and (f) to obtain

$$L/t_c = 0.866\,(1 - \alpha)(\sigma_{r,y}/\sigma_{c,y} - 1) \qquad (cc)$$

Figure 5. Approach to estimating order-or-magnitude of copper edge shear region, using simplified model.

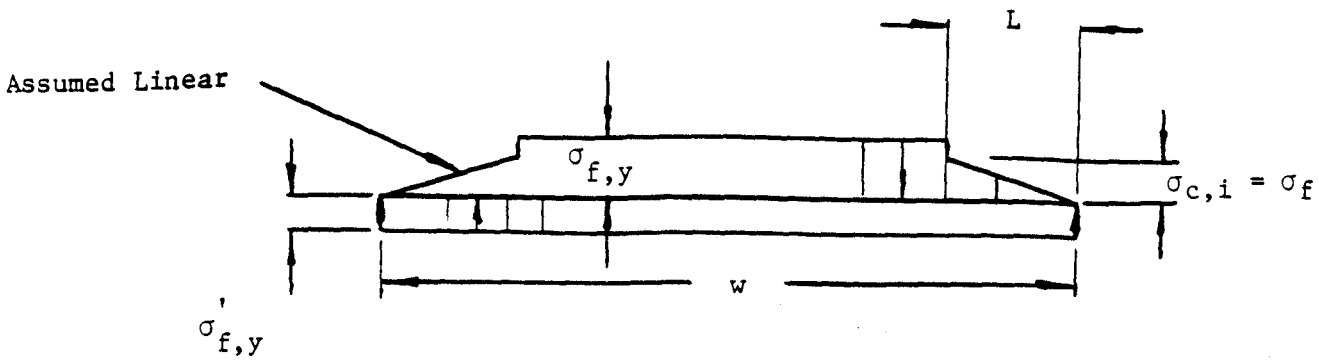

From face compression force balance,

$$\sigma'_{f,y} w = \sigma_{f,y}(w - 2L) + \sigma_{c,i} L \qquad \text{(dd)}$$

or

$$\sigma'_{f,y}/\sigma_{f,y} = 1 - (L/w)(2 - \sigma_{c,i}/\sigma_{f,y}) \qquad \text{(ee)}$$

From the mixture rule (e) and the tresca condition (f),

$$\phi = \sigma'_{f,y}/\sigma_{f,y} = 1 - (L/w)\,\frac{(1 + \alpha) + (1 - \alpha)(\sigma_{r,y}/\sigma_{c,y})}{\alpha + (1 - \alpha)(\sigma_{r,y}/\sigma_{c,y})} \qquad \text{(ff)}$$

Figure 6. Ratio ϕ, of effective face compression yield strength, $\sigma'_{f,y}$, to the mixture rule value, $\sigma_{f,y}$ for a finite width composite plane plate.

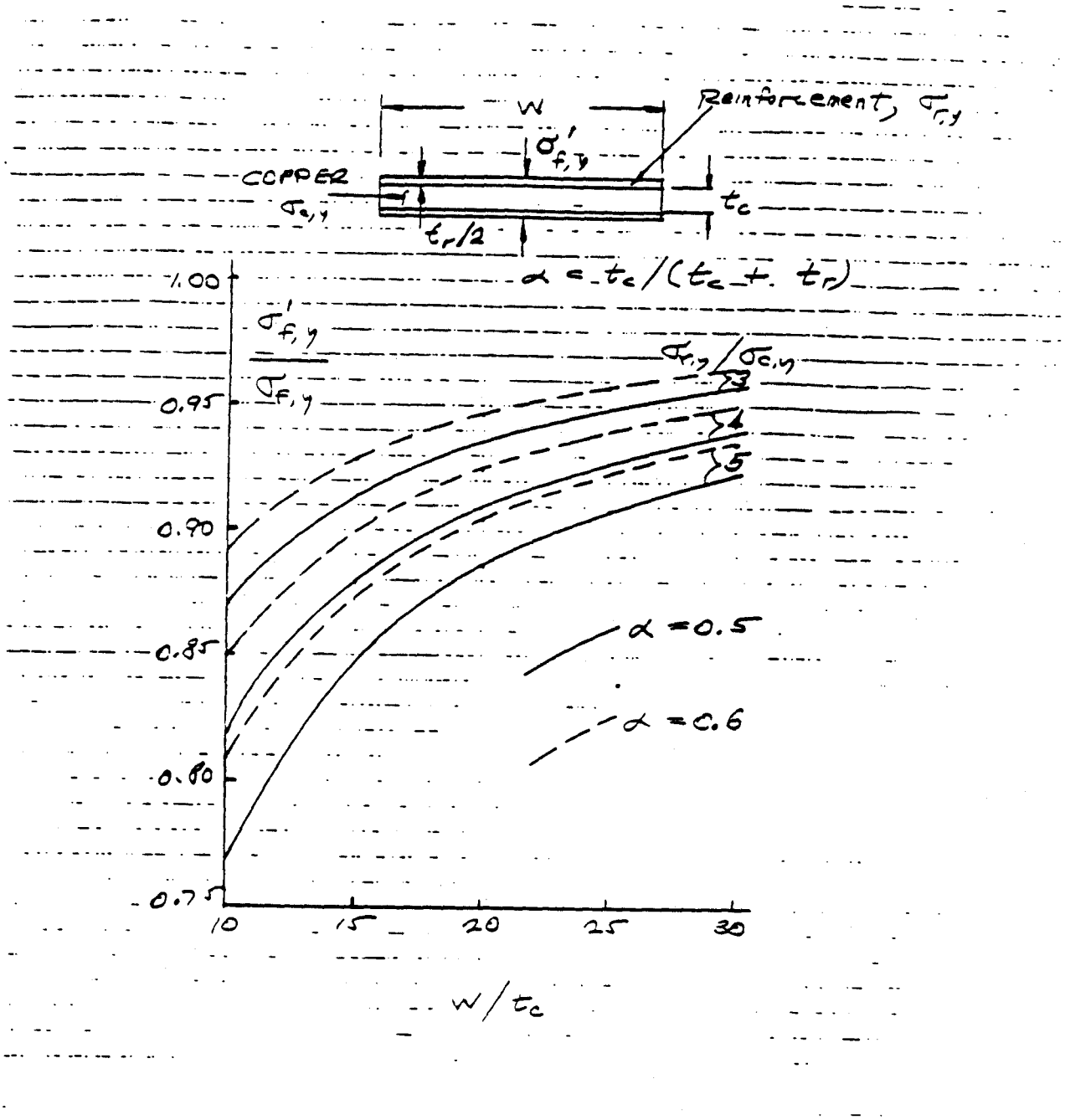

Figure 7. Sample curves of finite width correction factor.

TEST DATA AND DISCUSSION OF RESULTS

Introduction

Experimental results are presented, and are compared with predictions. There are many possible sources of inaccuracy in the measured behavior. Appendix 3 contains a discussion of some of those sources. It contains indications of the accuracies inherent in the load and deflection measuring devices, and identifies the possible role of specimen imperfections on observed specimen behavior.

The behavior of a face-compression composite depends upon compression stress-strain data in combination with inplane compression data for the copper, and with inplane tension data for the reinforcement. However, in this exploratory stage of the program it was convenient to confine the component material property testing to inplane tension. Compression testing of component material properties has been deferred to a later stage.

Specimen Structural Properties

The composite test specimen material and dimensional data appear in Table 1. Inplane tension stress-strain curves for the component materials are in the Appendices. They are the sources of the yield strengths and Young's moduli shown in the table.

TABLE 1

TEST SPECIMEN STRUCTURAL PROPERTY DATA

SPECIMEN[1]	COMPOSITION		t_c in (mm)	t_r in (mm)	w in (mm)	α	R	$\sigma_{c,y}$ ksi (MPa)	$\sigma_{r,y}$ ksi (MPa)	E_c msi (GPa)	E_r msi (GPa)
	BOND[2]	ARRANGEMENT[3]									
T1	R-B	C-S-C	0.110	0.037	0.60	0.75	5.5	——	——	30[7]	17[7]
T2	E-B	I-C-I[4]	0.255	0.245	0.20	0.51	0.78	40.0 (273)	129.9 (3954)	11.1 (131.0)	30.0 (227.5)
T3	E-B	I-C-I[5]	0.255	0.245	0.20	0.51	0.78	41.2 (284)	190.4 (1312)	19.1 (131.6)	30.4 (235)
T4	E-B	I-C-I[6]	0.255	0.245	0.20	0.51	0.78	16.4 (113)	166.7 (1149)	15.4 (106)	31.2 (215)
C1	R-B	C-S-C	0.110	0.037	0.60	0.75	5.5	——	——	——	——
C2	E-B	I-C-I[4]	0.255	0.245	2.0	0.51	7.8	See T2	See T2	See T2	See T2
C3	E-B	I-C-I[5]	0.255	0.245	2.0	0.51	7.8	" T3	" T3	" T3	" T3
C4	E-B	I-C-I[6]	0.255	0.245	2.0	0.51	7.8	" T4	" T4	" T4	" T4
C5	L	S-C-S	0.254	0.104	2.5	0.71	9.8	54.4 (375)	133 (917)	18.1 (125)	32.8 (226)
C6	L	S-C-S	0.086	0.104	2.0	0.45	23	46.0 (317)	133 (917)	17.4 (120)	32.8 (226)
C7	L	S-C-S	0.043	0.104	2.0	0.29	47	46.0 (317)	133 (917)	17.4 (120)	32.8 (226)
C8	L	S-C-S	0.086	0.104	2.0	0.45	23	7.0	133	17.4	32.8

1 T = Inplane tension specimen, C = face compression specimen

2 R-B = Roll bonded, E-B = explosion bonded, L = loose

3 I = Inconel 718, C = C-10100 copper, S = 301 stainless steel (I-C-I = Inconel faces, copper core, for example).

4 Solution annealed prior to cladding

5 Aged prior to cladding

6 Solution annealed prior to cladding, and aged after cladding

Inplane Tension Tests

Inplane tension stress-strain curves for the reinforced copper composites appear in Figs. 9 through 12. Yield strengths and moduli are presented in Table 2.

TABLE 2
COMPOSITE INPLANE TENSION TEST AND ANALYSIS RESULTS

SPECIMEN	FIGURE NUMBER	YIELD STRENGTH, $\sigma_{i,y}$, ksi (MPa)			YOUNG'S MODULUS, msi (GPa)			
		MEASURED	CALCULATED		MEASURED		CALCULATED	
			A	B	E_1	E_2	E_1	E_2
T1	9	86.6	1	1	20.3	—	20.3	—
T2	10	79.2	82.0	83.9	20.5	—	23.4	—
T3	11	99.7	108.0	114.3	21.0	—	24.7	—
T4	12	88.3	88.3	90.4	20.4	15.9	23.1	15.2

A From the prediction (dashed curve) determined by calculating $\sigma_{comp} = \alpha\sigma_c + (1 - \alpha)\sigma_r$ at selected strains on the component stress-strain curves in Appendix 1.

B From the mixture rule $\sigma_{i,y} = \alpha\sigma_{c,y} + (1 - \alpha)\sigma_{r,y}$ using the yield strengths shown in Table 1.

1 Steel stress-strain curve not available at strains in the yield region. Specimen too small to grip properly.

All theoretical curves were constructed from the parallel mixture rule

$$\sigma_{comp} = \alpha\sigma_c + (1 - \alpha)\,\sigma_r \qquad (10)$$

which was applied at several strains to obtain the starred curves shown on Figs. 9 through 12. In addition, primary moduli were calculated from

$$E_{i,1} = \alpha E_c + (1 - \alpha)E_e \qquad (11)$$

Secondary moduli (for low-yield-strength copper) was found from $E_{i,2} = (1 - \alpha)E_r$. However, only T4 exhibited a secondary modulus (Fig. 12). For the other composites, the copper strains at 0.002 offset yield were within the yield region of the reinforcements, which prevented identification of a secondary modulus.

The T1 modulus and tension yield strengths agreed well with the predictions if assumed values for $\sigma_{c,y}$ and $\sigma_{r,y}$ are 50 ksi (345 MPa) and 200 ksi (1380 MPa) for the heavily cold rolled R-B strip. The component properties could not be measured. The measured values for the E-B I-C-I specimen were somewhat below the predictions. It is conceivable that the interface wave may have been a factor, since the effect of the reinforcement stiffness bond strengths would be less than the average perpendicular to the waves and greater than the average parallel to the waves, causing orthotropic behavior instead of isotropic behavior (Fig. 8). This condition did not exist in the roll-bonded specimen, T1, for which theory agreed well with experiment. The wave-induced orthotropicity also may have affected the behaviors of the face-compressed stacks.

The possibility of a wave effect requires measurement of E-B component and composite properties parallel and perpendicular to the wave directions, which was not done in this phase of the test program.

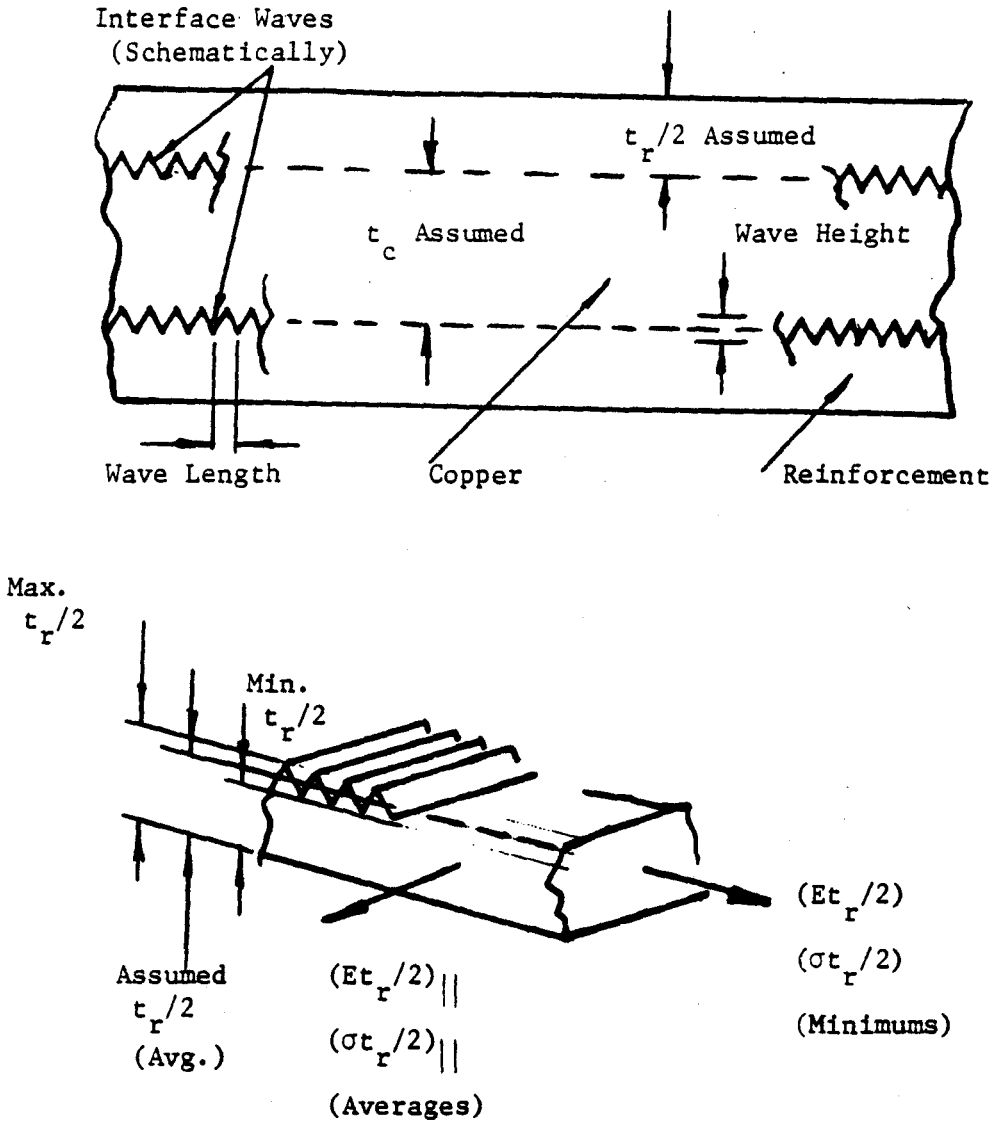

Figure 8 Effect of interface wave on explosion-bonded composite stiffness and strength.

Face Compression Tests

Perhaps one of the most important features of the face compression tests was the observation that the face compression yield strengths were greater than the copper yield strengths (a ratio of 8/1 for C8). Another important feature was the inability to detect visually any indication of large bulging of the copper at the plate edges. At the most, it appeared to be of the order of a few thousandths of a inch (possibly as much as 0.010 inch), including stack C5 which was loaded to 4.4 percent face-compression strain. That observation would seem to bolster the view that copper yielding is inhibited by the reinforcement.

The face compression tests were performed on stacks of composite with no insulation between plates (except for C4 for which the plates were cemented together). The tests data and predictions appear in Table 3. The yield strengths and Young's moduli were obtained from the stress-strain curves in Figs. 13 though 20.

The eight stack face compression tests produced an average ratio, $\mu = 1.05$, of measured effective yield strength to theoretical effective yield strength, $\phi = \sigma'_{f,y(meas)}/\sigma'_{f,y(calc)}$. The standard deviation ($\Sigma[x_i - \mu]^2/8$, was 0.03.

TABLE 3

FACE COMPRESSION RESULTS

SPECIMEN	$\sigma'_{f,y(calc)}$ [1] psi(MPa)	$\sigma'_{f,y(meas)}$ psi(MPa)	$\frac{\sigma'_{f,y(meas)}}{\sigma'_{f,y(calc)}}$	$\sigma_{i,y(meas)}$	$\frac{\sigma'_{f,y(meas)}}{\phi\sigma_{i,y(meas)}}$	$E_{(meas)}$ msi(GPa)	$E_{(calc)}$ msi(GPa)
C1	72 (497)[2]	72 (497)	1.00	87 (600)	1.01	11.4 (79)	19.8 (137)
C2	69 (476)	67 (462)	0.98	79 (545)	1.07	13.4 (92)	23.4 (161)
C3	83 (572)	91 (628)	1.10	100 (690)	1.25	17.0 (117)	23.2 (160)
C4	39	45 (310)	1.15	88 (607)	1.18	18.6 (124)	23.1 (159)
C5	72 (497)	66 (455)	0.92			20.1 (139)	22.4 (154)
C6	87 (600)	89 (614)	1.02			17.1 (118)	25.9 (179)
C7	104 (717)	106 (731)	1.02			20.5 (141)	28.3 (195)
C8	48 (331)	59 (407)	1.23			8.1 (56)	25.9 (179)
			====				
			1.05 ± 0.03				

[1] $\sigma'_{f,y(calc)} = \phi\sigma_{f,y}$; ϕ = finite width correction factor from Eqs. (8) and (9); $\sigma_{f,y}$ = mixture rule yield strength from Eq. (7).

[2] Estimate, using $\sigma_{c,y}$ = 50 ksi (345 MPa) and $\sigma_{r,y}$ = 200 ksi (1380 MPa) from tension test.

The Young's moduli were derived from the linear regions of the stress-strain curves. The low values (relative to the theoretical value) may have resulted from the often-observed phenomenon of interface effect between plates. It could consist of general out-of-flatness and nonuniform thickness of the stack plates possibly augmented by surface roughness of each plate face. The relatively flat initial portion of the stress-strain curves for C2 and C3 (Figs. 14 and 15) may reflect the influence of those phenomena. The variations of initial slope among the eight face compression stack curves could indicate the uncertainties in the magnitudes of those influences.

The first two runs on C5 (Fig. 17) indicate good reproducibility of the "linear" slope at 19.3 msi (133 GPa), which is 94% of the theoretical value of 20.5 msi (150 GPa). However, the initial nonlinearity persisted in all three runs. The curve for the third run had an elastic-region slope of 17.7 msi (122 GPa). That change from the 19.3 msi value may have been due to use of the single extensometer, in addition to the other stack imperfections. In any case, it is 86% of the theoretical value.

The composite stress-strain curves do not appear to indicate secondary modulus behavior. Nonlinear behavior of C4 (Fig. 16) did not begin before 20 ksi (138 MPa), which is well beyond the copper yield of 16.4 ksi (113 MPa) in that plate.

Table 3 shows that most of the measured face compression yield strengths exceeded the predicted values. That reveals inaccuracy in the edge correction factor, ϕ, and in the mixture rule strength calculation, $\sigma_{f,y}$. The two specimens, C6 and C7, had large aspect ratios ($R = w/t_r$)

and high copper yields relative to the reinforcement. They revealed specimen yield strengths close to $\sigma_{f,y}$. However, the C8 yield was 23 percent above prediction with R = 23, but with $\sigma_{r,y}/\sigma_{c,y}$ = 17.5. If C6 and C7 can be assumed to substantiate the mixture rule (which applies to an infinite plate), then the 23 percent error may be an overestimate of the edge correction factor, ϕ. A similar situation occurred for C4 (with $\sigma_{r,y}/\sigma_{c,y}$ = 9.6, α = 0.51 and w/t_c = 7.8) which exhibited a face compression yield strength 15 percent above the predicted value. Those cases were balanced by C2 and C5, for which the measured strengths were below prediction.

The results from C1 through C8 appear to indicate that $\sigma'_{f,y}/\sigma_{f,y}$ increases with $\sigma_{r,y}/\sigma_{c,y}$. It may be argued that 8 tests are two few to permit reliable identification of trends. In any event, it is clear that more study of ϕ is warranted. It also follows that only test data on full scale configurations should be used for final design.

Specimen C5 was loaded beyond yield in an attempt to determine the nature of a possible compression failure mode. At 80 ksi (552 MPa) the test was stopped. The strain was 0.044, which approached the 5% limit of the extensometer. Also, the specimen exhibited the onset of buckling, which was anticipated to be one possible failure mode. The observed half-cosine buckle shape, and approximate slope of the stress-strain curve (0.2 msi, or 1.4 GPa), provided reasonable correlation of the observed value with an order-of-magnitude estimate of the plastic critical stress.

Table 3 indicates that $\sigma'_{f,y}$ may be equal to, or greater than, the product of the inplane tension yield and the edge correction factor, $\phi\sigma_{i,y}$. Again, it may be too early to define trends.

CONCLUSIONS

1. The copper cannot begin to display large strains that are associated with yielding until the reinforcement does so.

2. Composite tension stress-strain curves can be constructed with reasonable reliability using the mixture rule

$$\sigma_i = \alpha\sigma_c + (1 - \alpha)\sigma_r$$

at several simultaneous strain levels on the copper and reinforcement stress-strain curves. Young's moduli and yield can be measured on the constructed curve. However, the reliability of the procedure might be degraded for an E-B composite if the interface wave height is a large fraction of the thickness of either component.

3. Composite face compression yield strength apparently is determinable by using the mixture rule for an infinite plate,

$$\sigma_{f,y} = \alpha\sigma_{c,y} + (1 - \alpha)\sigma_{r,y}$$

together with the finite width correction factor, ϕ, shown in Eqs. (8) and (9).

4. Inplane tension yield strength of a narrow composite strip should agree with compression yield strength of an infinite plate composite if the finite width correction factor is applied to the inplane value.

5. More testing is required to broaden the data base from which those conclusions were drawn.

DESIGN EXAMPLE

Assume that a tapered plate of the CIT TF coil can be modeled at the throat region as a constant-thickness plate with t_c = 0.375 in (9.52 mm) and t_r = 0.250 in (6.35 mm). Assume, also, that those dimensions occur in the midsection of the 7.55 in (192 mm) tapered zone, so that w = 3.775 in (95.88 mm). Then α = 0.60 and w/t_c = 10. If the inconel yield strength is 177 ksi (1218 MPa) and that of the copper is 44.7 ksi (308 MPa) at 293 K, then $\sigma_{r,y}/\sigma_{c,y}$ = 4.

Enter Fig. 7 (repeated on the following page) with $\sigma_{r,y}/\sigma_{c,y}$ = 4, α = 0.6, and w/t_c = 10. It is found that ϕ = 0.85. From the mixture rule,

$$\sigma_{f,y} = 0.6\text{x}44.7 + 0.4\text{x}177$$
$$= 97.6 \text{ ksi } (673 \text{ MPa})$$

then

$$\sigma'_{f,y} = \phi\sigma_{f,y} = 0.85\text{x}97.6$$
$$= 83.0 \text{ ksi } (572 \text{ MPa})$$

If the allowable stress were to be chosen at 85% of yield, then

$$\sigma_{all} = 0.85\text{x}83.0$$
$$= 70.6 \text{ ksi } (487 \text{ MPa})$$

The above calculation may be conservative since the actual plate width is twice the value arbitrarily selected for the example. A full scale test on an actual plate would be required to identify the real behavior.

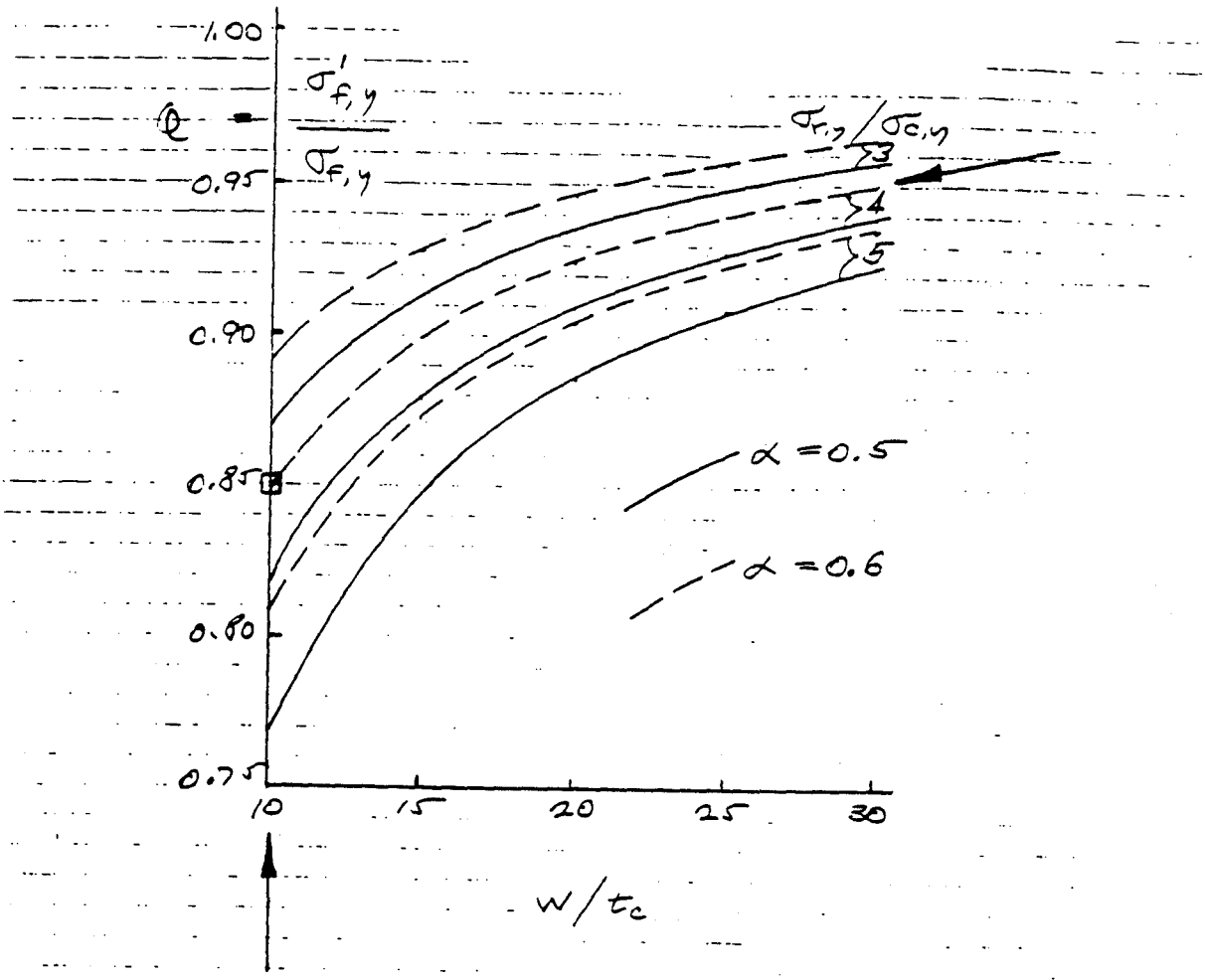

Figure 7. (Repeat) Use of finite width correction in a sample problem.

APPENDIX 1

INPLANE TENSION
STRESS-STRAIN CURVES

NOTE: Tension stress-strain curves for composite components are displayed on Figs. 10, 11, and 12.

The stress-strain curves in this report were generated by straight line segments joining load-deflection data points (scaled appropriately) as measured by the various testing machines at MANLAB, INC. The plots were produced by Graph__MG, a graphic package installed on the MIT Alcator Vax.

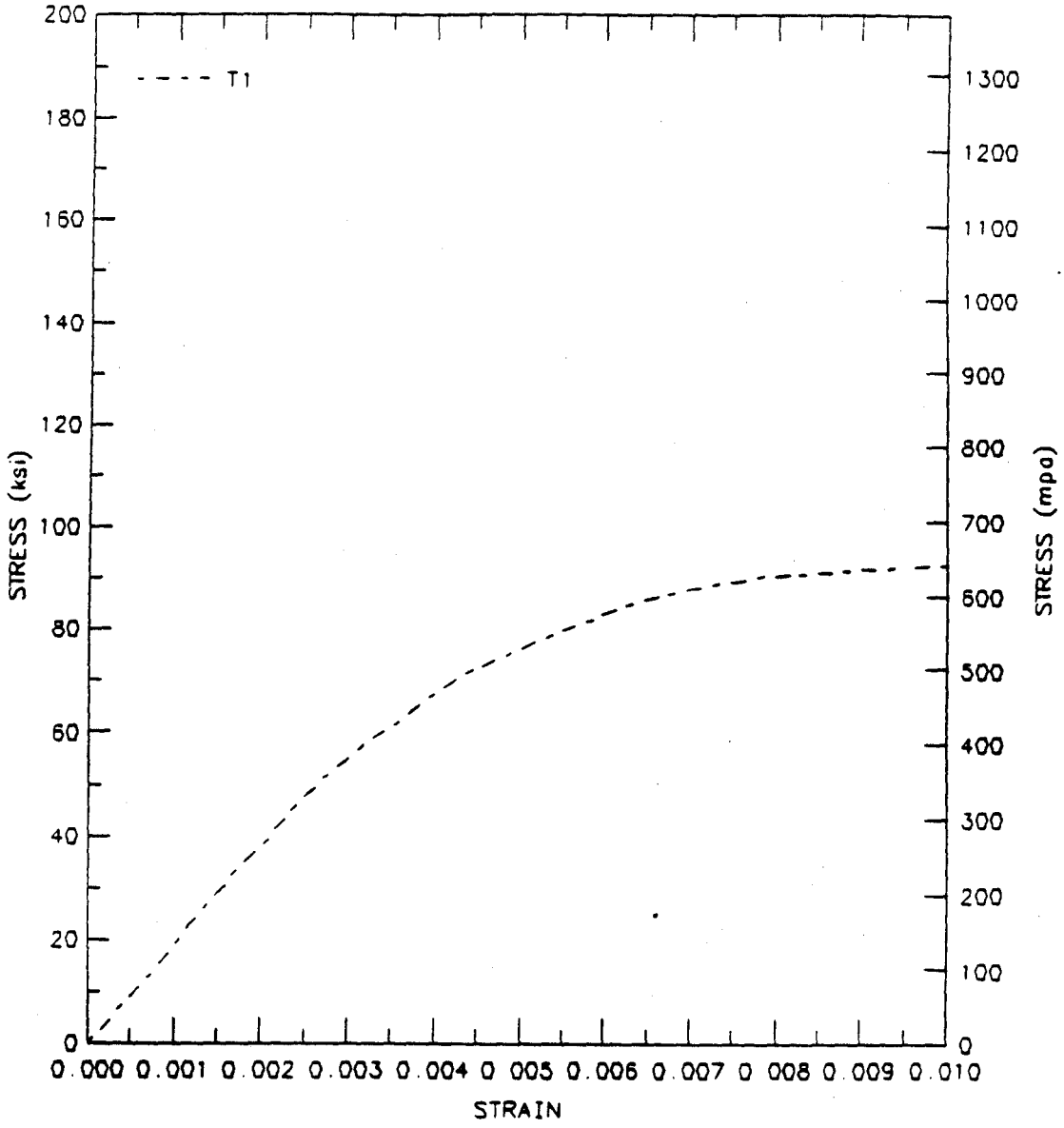

Figure 9. Inplane tension stress-strain curve for Specimen T1

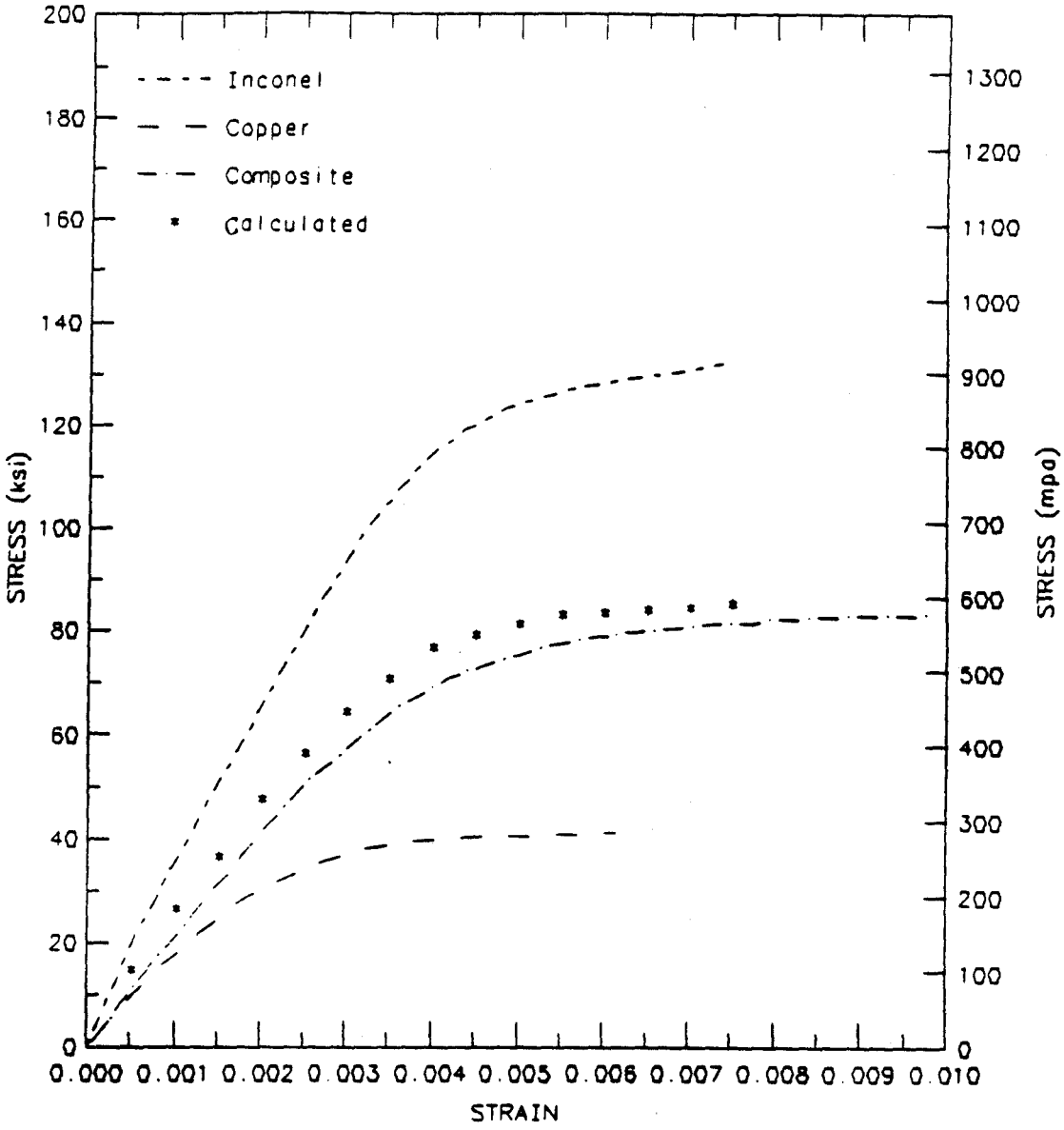

Figure 10. Measured and calculated inplane tension stress-strain curves for Specimen T2

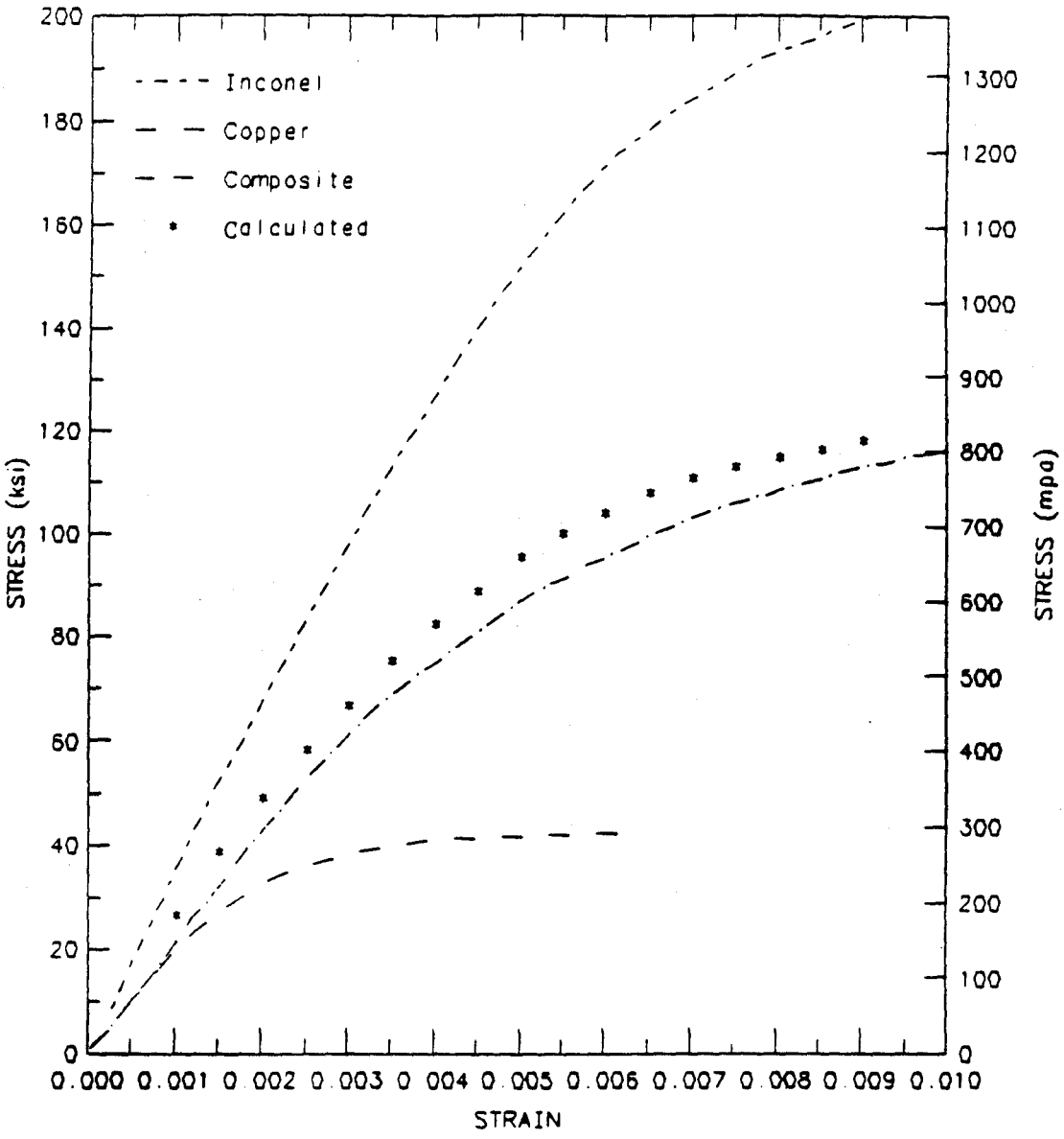

Figure 11. Measured and calculated inplane tension stress-strain curves for Specimen T3

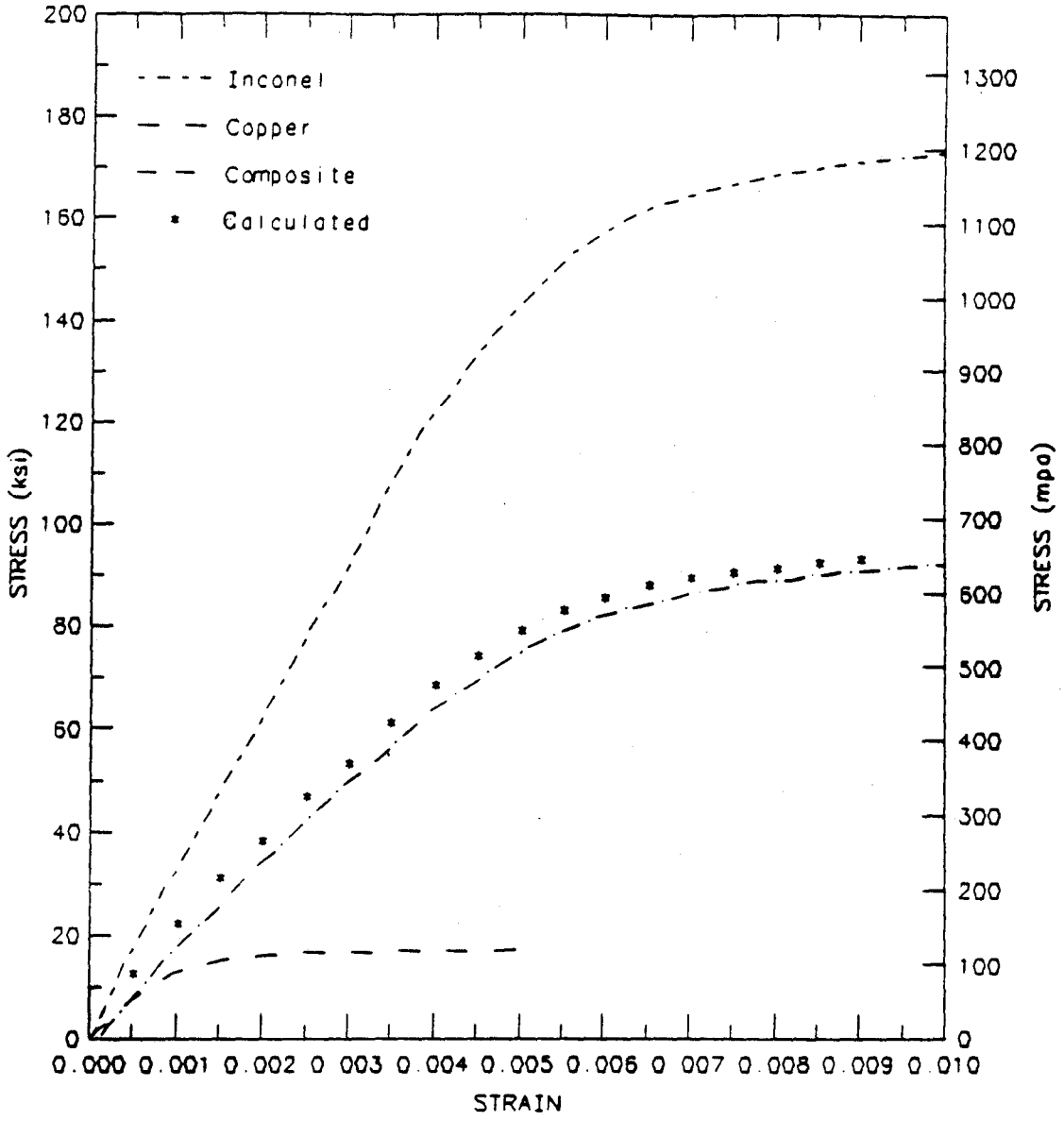

Figure 12. Measured and calculated inplane tension stress-strain curves for Specimen T4

APPENDIX 2

FACE COMPRESSION
STRESS-STRAIN CURVES

(NOTE): Tension stress-strain curves for composite components are displayed on Figs. 14 through 20).

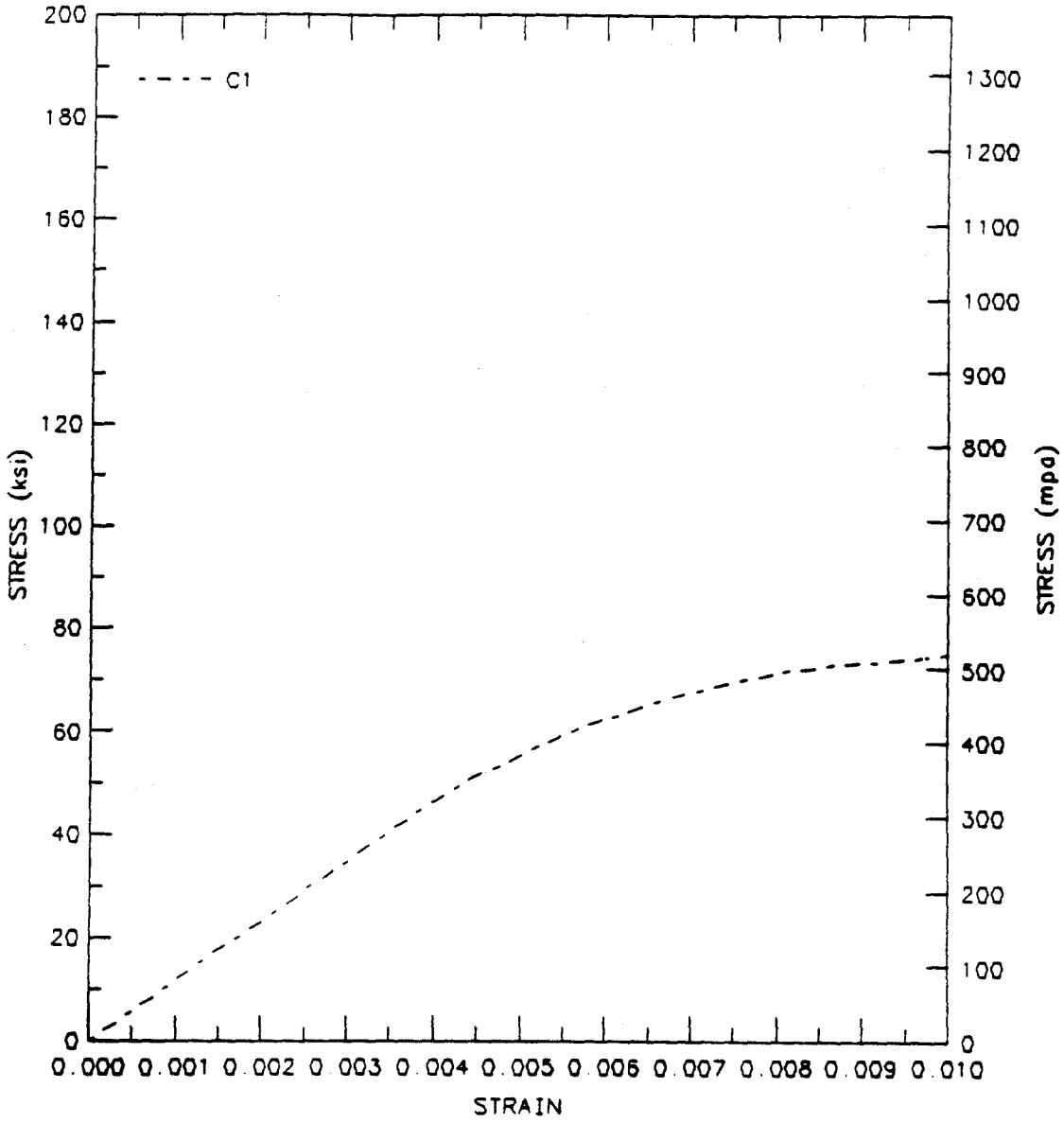

Figure 13. Measured face compression stress-strain curve for Specimen C1

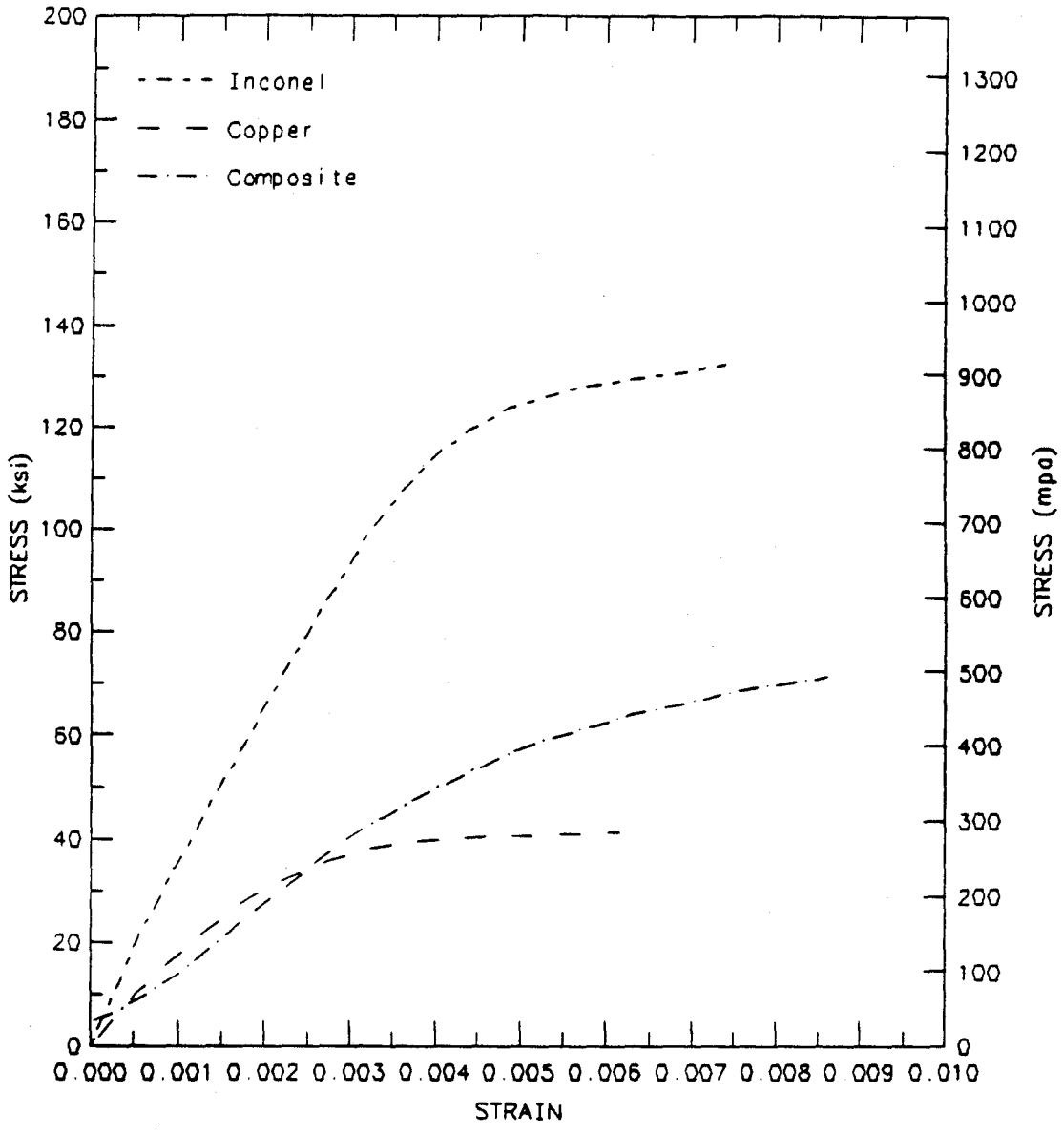

Figure 14. Measured face compression stress-strain curve for Specimen C2

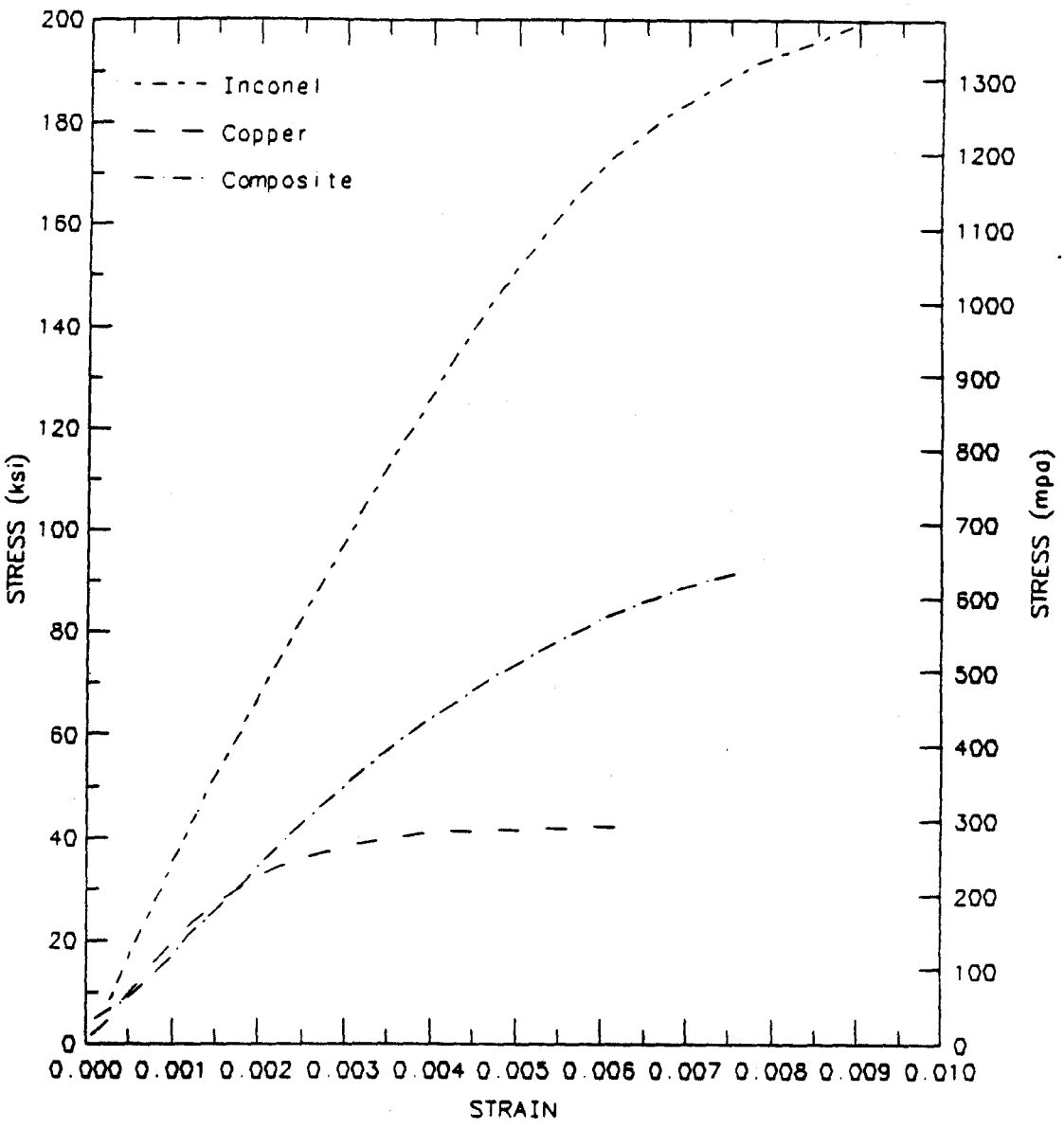

Figure 15. Measured face compression stress-strain curves for Specimen C3

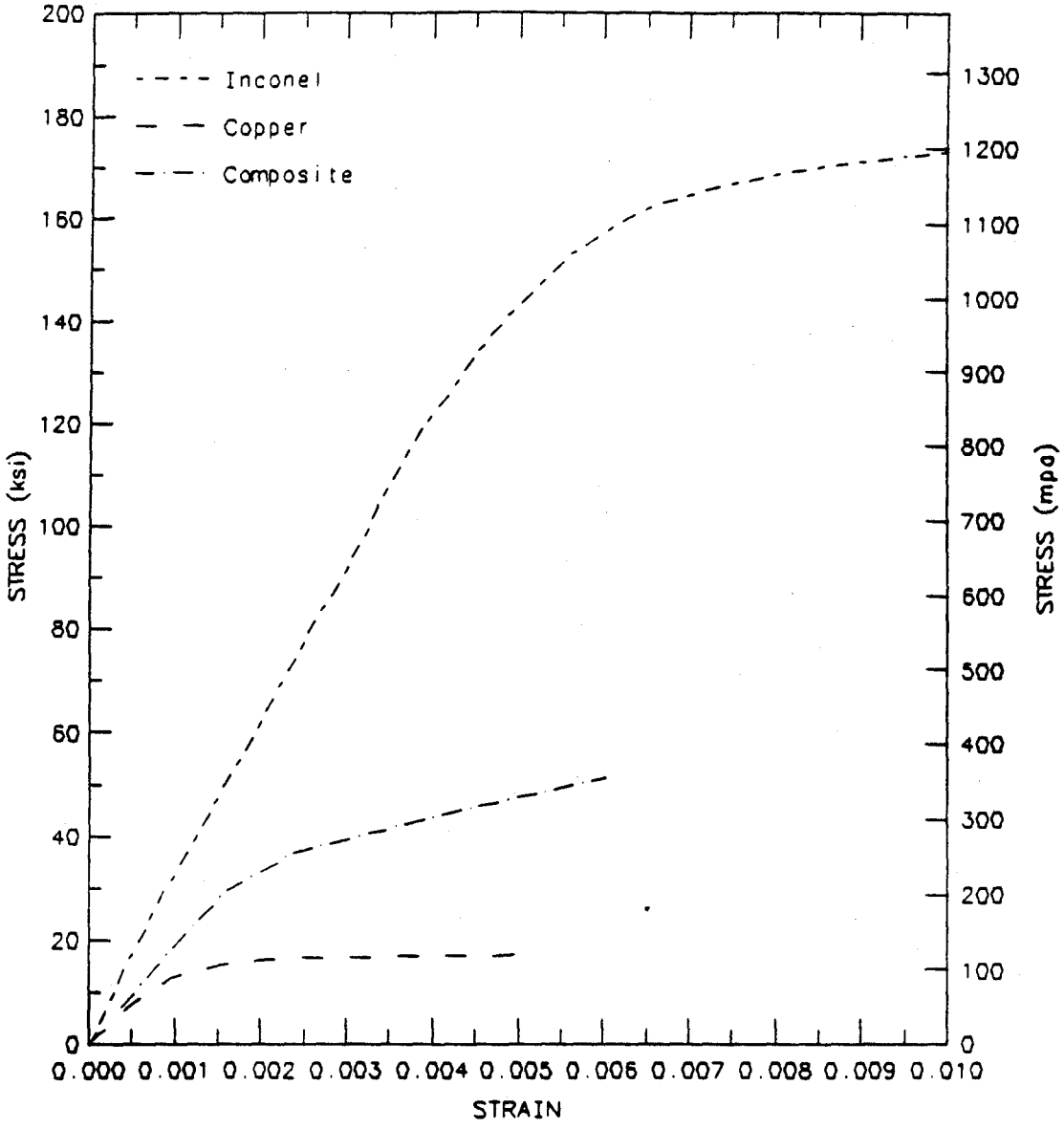

Figure 16. Measured face compression stress-strain curve for Specimen C4

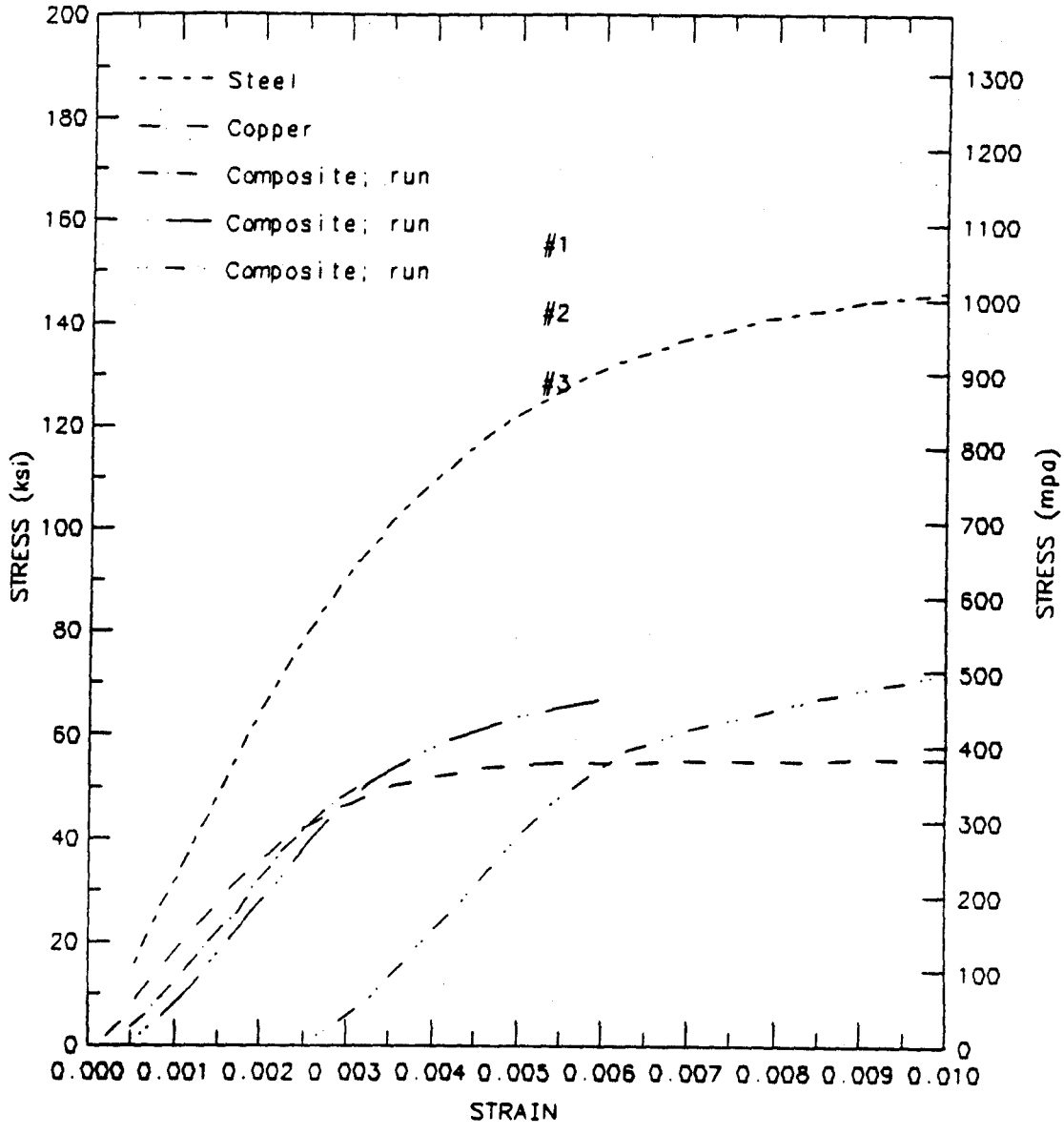

Figure 17. Measured face compression stress-strain curve for Specimen C5

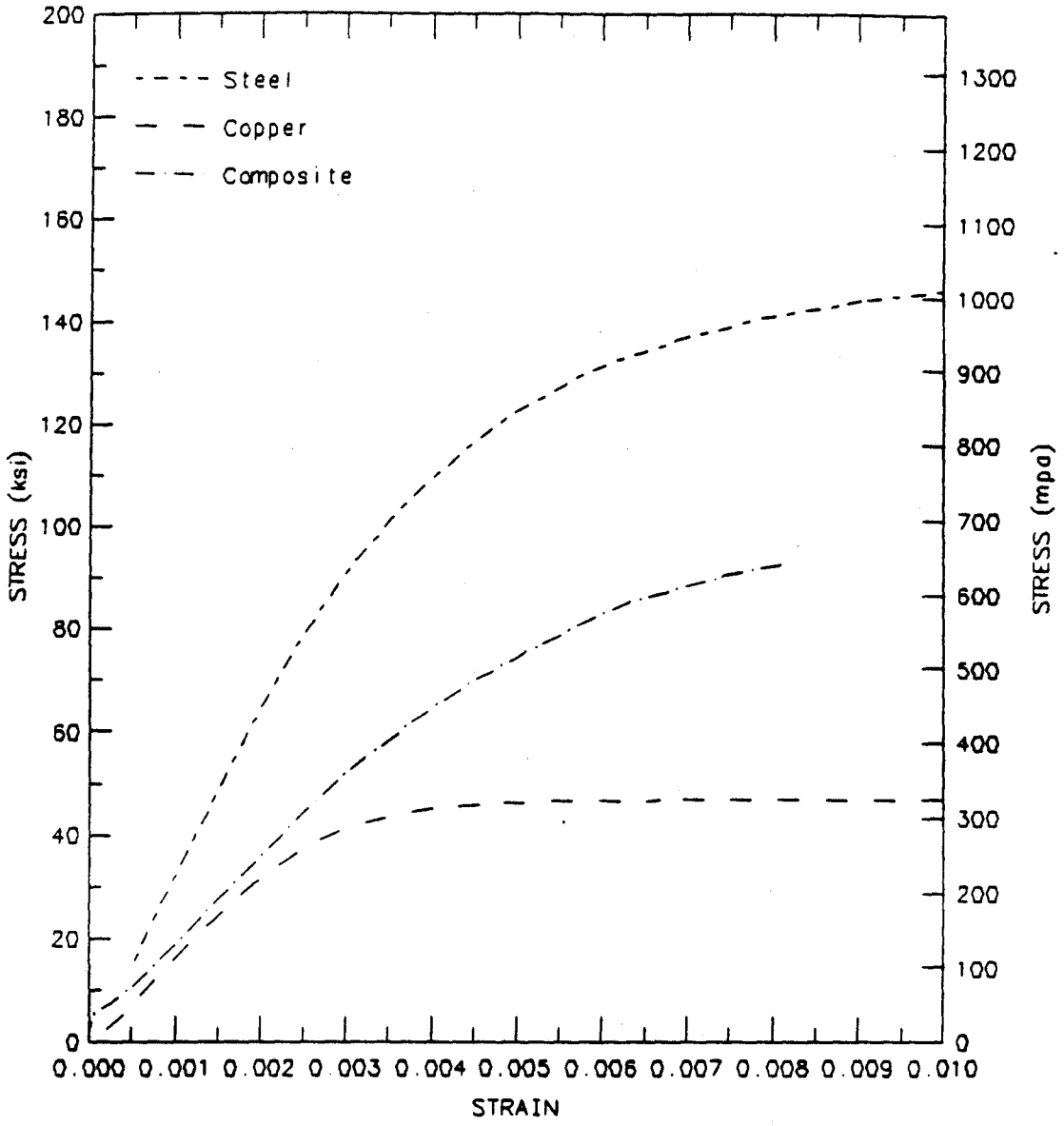

Figure 18. Measured face compression stress-strain curve for Specimen C6

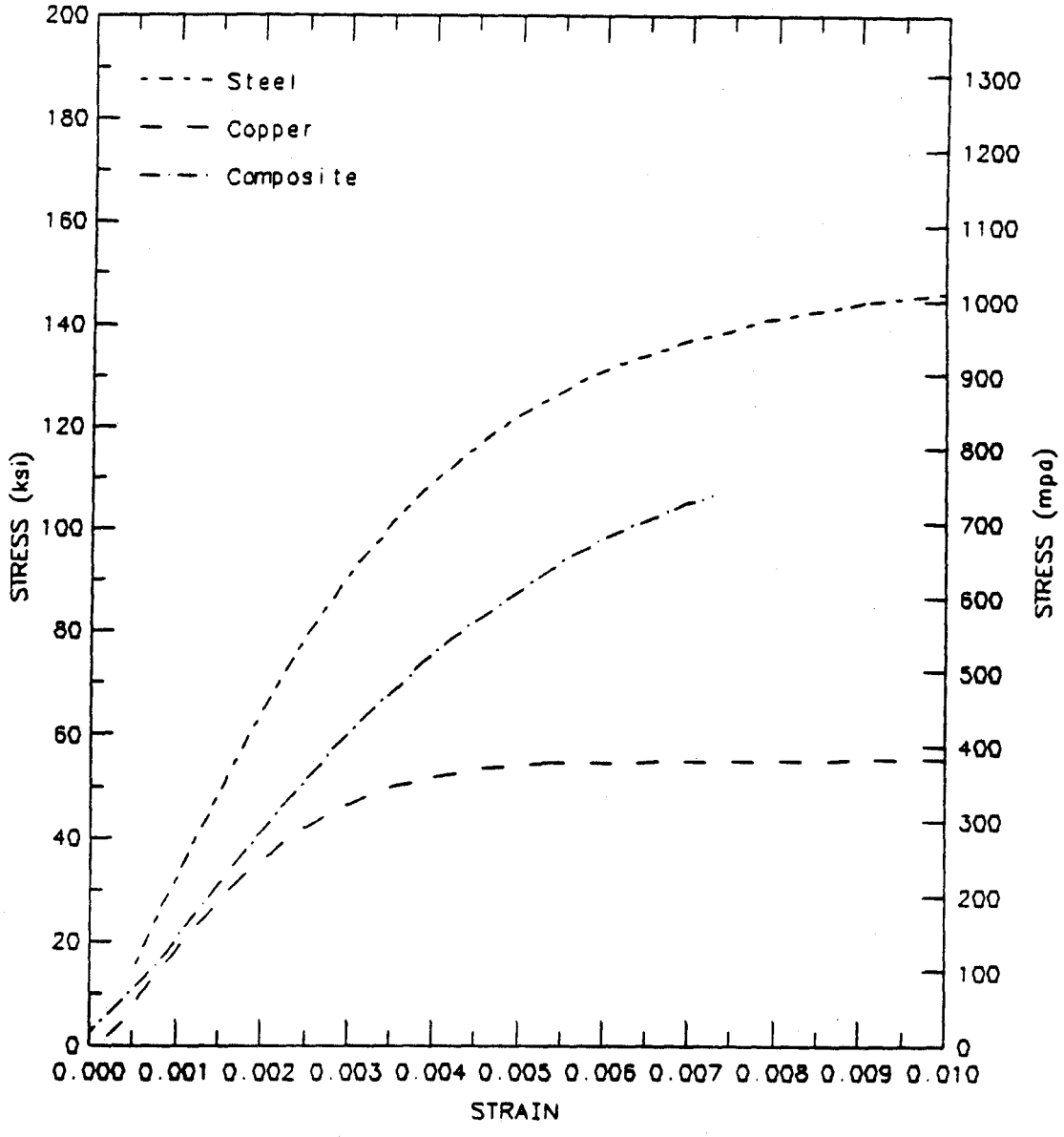

Figure 19. Measured face compression stress-strain curve for Specimen C7

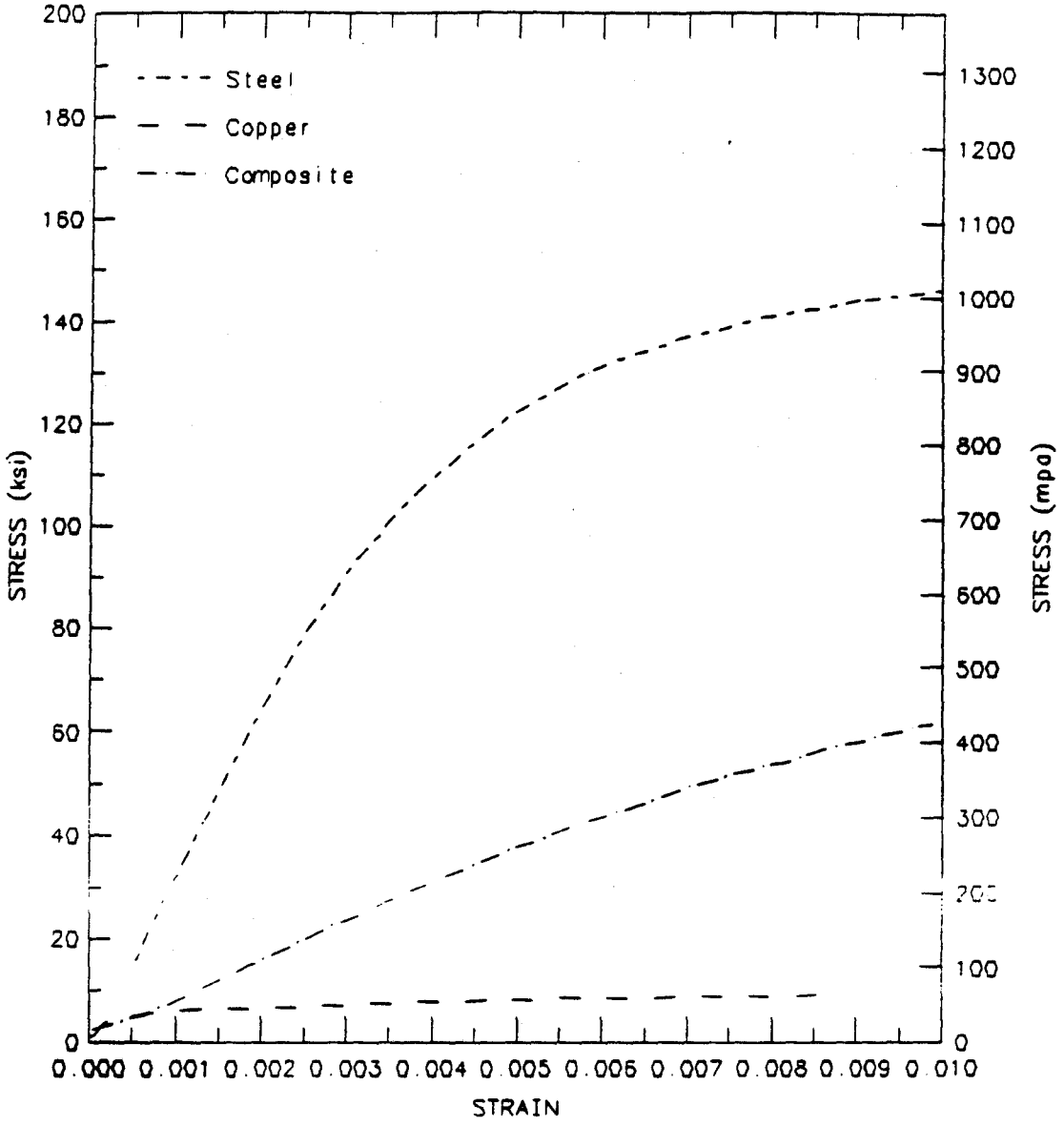

Figure 20. Measured face compression stress-strain curve for Specimen C8

APPENDIX 3

SOURCES OF TEST INACCURACIES

Force Measurement

The various tests were performed in several machines at Manlabs. Their Mlb (7 MN) and 0.3 Mlb (2 MN) presses were used to apply face compression to the stacks. The 60,000 lb (0.4 MN) Baldwin Universal Tester and the 20,000 lb (0.14 MN) MTS testing machine were used for loading composites and composite components in tension. All the machines were calibrated to an accuracy of better than one-half percent throughout the respective load ranges. The minimum direct reading on the Mlb press was 2,000 pounds. It was 1,000 pounds on the 0.3 Mlb press. They were noted visually and recorded. The loads on the other two machines were displayed as ordinates on the X-Y recorder used to acquire load deflection data. The precision was 10 pounds on the Baldwin and 20 pounds on the MTS.

The crossheads on the presses were not free to swivel, which could have caused some unevenness in pressure across a stack face. The anvil faces were ground, and were oriented parallel, as closely as possible. Also, several sheets of fiberglass were inserted between each loading anvil and stack face to help distribute the load evenly across a stack face.

Deflection Measurement

Compression deflections were measured with an Instron one-inch gauge-length extensometer which senses movements that are multiples of 10^{-5} inch. They are displayed digitally for hand recording. Tension deflections were acquired as the abscissa of the X-Y recorder. The precision was 4×10^{-4} inch on the Baldwin recorder and 10^{-4} on the MTS. The extensometers were calibrated several times during the program and were found to agree with the reference micrometer that read to 10^{-4} inch.

Effects of Specimen Imperfections

The force and deflection measurement accuracies presumably were good enough to provide reliable data on specimen behavior. It is likely that specimen imperfections led to such stress-strain curve features as nonlinearity at low stresses and deviations of measured Young's moduli from commonly reported values. The extensometers were mounted on one side of each specimen. That could result in a nonlinear stress-strain curve for a thin strip that was not perfectly flat, or that was not gripped properly in the testing machine. In a compression stack, tolerances could be built up making one stack edge higher than another. Plate waviness (particularly in explosion-bonded plates) could have been the cause of uncertainties in Young's modulus values, and also may have affected 0.002 offset yield strengths. The Specimen C4 plates, for example, were found to be as much as 0.012 inch (1/3 mm) out of flat relative to the edges of the 2-inch squares from which the stack was constructed.

The interface waves on the E-B plates made it difficult to measure reliably the thicknesses of the components in the composite. The midline of the wave was chosen for that purpoose. It was identified by magnification of a region polished as for metallurgical analysis. That thickness agreed to a few percent with the value obtained by removing the copper from an Inconel face strip, weighing the strip, and calculating the volume using the specific gravity of the Inconel as obtained from a flat strip. It is not known how that geometric thickness relates to the "structural" thickness of the component in a composite. Furthermore, the effective thickness for inplane loads parallel to the wave ridges would be greater than the effective thickness for inplane loads across the ridges. That would lead to orthotropic structural behavior in both stiffness and strength.

APPENDIX 4

FUTURE PROGRAM

The test data and theory/experiment correlations in this report are encouraging, but only can be considered preliminary. The specimens were smaller than the full scale dimensions of CIT TF coils. Full scale E-B plates have not yet been produced. All tests were performed at 293 K under short-time static load. All component stress-strain curved were obtained in inplane tension although the stack tests were conducted in face compression. Compression stress-strain data must be obtained. It is necessary to determine the impact on E-B properties of scale, elevated temperature, and cyclic loading. E-B bond strength must be measured. Future goals will be addressed to those problems. In addition, the role of insulation must be explored.

Face compression tests will be performed on stacks with several widths in the range from 100 to 200 mm. A few preliminary creep tests have been performed and will be reported shortly. Cyclic compression and tension tests will be performed, simulating CIT performance. Stacks of copper plates and inconel plates will be compressed to obtain Young's modulus and yield strength data for the composite components. Bond shear strength will be measured in combination with various amounts of face compression, for which a test specimen has been designed. Tension and compression tests will be performed at 393 K. Throughout the program, the effect of insulation on face-compression behavior will be studied.

Prediction methods will be reviewed critically, and limitations of use will be identified. Inevitably, there will be feedback from the magnet design activities, which may require parameters outside the range of parameters explored to date and currently planned for the additional tests.

REFERENCES

1. Internal memorandums to MIT from Teledyne Engineering Services, 1980.

2. D.R. Cohn, et al., "Engineering Design Considerations for Compact Ignition Test Reactors," PFC Report PFC/CP-81-2, February 26, 1982.

3. M. Leupold, "Strength Tests of Composite Structures as Applied to High Field Magnet Windings." MIT FBNML memorandum, January 24, 1966.

4. P.W. Bridgman, "The Physics of High Pressure," G. Bell and Sons, London, 1949.